KSCE Journal of Civil Engineering (2016) 20(4):1356-1364
DOI 10.1007/s12205-015-0635-2


Railroad Engineering
pISSN 1226-7988, eISSN 1976-3808
www.springer.com/12205

# Static and Dynamic Behavior of Transitions between Different Railway Track Typologies

**T. Real*, C. Zamorano**, C. Hernández***, J. A. García****, and J. I. Real*******

Received Octber 27, 2014/Revised February 25, 2015/Accepted May 27, 2015/Published Online August 31, 2015

**Abstract**

A railway track stretch comprising three different track typologies (i.e., ballasted track, asphalt slab track and concrete slab track) has been modeled using a three-dimensional Finite Elements model, which has been calibrated and validated using real acceleration records. In this model, two different analyses have been run: a static analysis to assess the stiffness evolution and a dynamic analysis to calculate the accelerations induced by the train loads along the transition zones. These analyses have been used to assess the performance of three different techniques existing in the literature to improve the structural behavior of the track in the transition areas: the variation of the stiffness of the elastomers, the implementation of additional rails and the use of resilient mats. Results have demonstrated that these techniques perform generally better in the track vertical stiffness transition between the concrete and asphalt slab tracks while the dynamic response is not significantly altered in any scenario.

Keywords: *railway transition, FEM, railway vibrations, track vertical stiffness, asphalt slab track*

## 1. Introduction

Changes in vertical stiffness exist in all the railway lines. If these changes are too sudden, they can produce dynamic effects affecting track durability as well as passengers' comfort. As a consequence of the recent improvements in railway networks design, many resources have been invested in the study of transitions, putting forward solutions to smooth the stiffness variations in order to minimize their negative effects.

Coelho *et al.* (2011) point the execution of a gradual stiffness change as the key aspect to reduce the undesirable consequences of the transitions. Additionally, these authors monitor a culvert and state that the variation of the stiffness over the life span of the track must be considered to achieve a proper design, paying special attention to the settlements produced in the different layers of the infrastructure. The problem in the culverts was also experimentally studied by Li and Davis (2005) who analyzed four railway bridges with stiffness changes up to 200% and demonstrated that the larger deterioration rate of the granular layers and the higher ratio of cracked sleepers are produced near the transition zone. Xia *et al.* (2010) offered numerical data from the monitoring of a railway bridge, setting an influence zone in which abnormal deflections and accelerations are produced within a distance of 15-20 m before the abutment. A minimum value of 150 MPa for the elasticity modulus of the materials in the granular layers was also established for the good performance of the transition.

Models based on the Finite Elements Method (FEM) have become an extremely useful tool for the study of railway transitions. In this regard, it should be mentioned the work of Zhang *et al.* (2013) who predicted the response of the system vehicle-track in a transition using a multibody FEM model when the operating speed of the line was increased up to 200 km/h. The results showed that while the vehicle accelerations remained behind the limits, the wheel-rail contact forces were enlarged as a consequence of the high speed. Analogously, Shi *et al.* (2012) predicted the behavior of a bridge-embankment transition in a future scenario in which the load per axis transmitted was augmented using a 3D FEM model validated with real data from the transition. Varandas *et al.* (2011) also used complex numerical methods for the vehicle-track system over a culvert, evidencing the variability of the contact forces between the sleeper and the ballast as a consequence of the severe deterioration of the granular material in transitions.

Apart from describing the phenomenon and predicting future

*Researcher, University Institute for Multidisciplinary Mathematics, Polytechnic University of Valencia, 46022 Valencia, Spain (Corresponding Author, E-mail: tereaher@upv.es)
**Researcher, Foundation for the Research and Engineering in Railways, 160 Serrano, 28002, Madrid, Spain (E-mail: claraz@fundacioncdh.com)
***Researcher, University Institute for Multidisciplinary Mathematics, Polytechnic University of Valencia, 14 Camino de Vera, 46022 Valencia, Spain (E-mail: cehergra@cam.upv.es)
****Researcher, Ferrocarrils de la Generalitat Valenciana (FGV) 46014, Valencia, Spain (E-mail: garcia_juacere@gva.es)
*****Head Researcher at University Institute for Multidisciplinary Mathematics, Polytechnic University of Valencia, 46022 Valencia, Spain (E-mail: jureaher@tra.upv.es)

scenarios, FEM can be used to design strategies to reduce the negative effects produced at the transitions. For instance, Gallego Giner *et al.* (2012) justify the use of granular materials reinforced with cement to avoid the sharp stiffness changes employing a FEM model and Witt (2008), who uses the FEM to assess the influence of the under sleeper pads in zones where the track vertical stiffness changes. Other solutions have been directly tested in real tracks as the ballast coating using polyurethane geocomposites to minimize the degradation of the ballast layers in transition zones (Woodward *et al.*, 2012).

In this paper, two different transitions between three different track typologies (ballasted track, concrete slab track and asphalt slab track) are analyzed. This transition has already been designed and executed in a real track, so real acceleration registers will be used to construct a 3D FEM model to study new strategies to smooth the stiffness changes among the three different tracks. The importance of the transitions between different track typologies was studied by Ali Zakeri and Ghorbani (2011) who demonstrated the benefits of introducing a concrete slab under the ballast in the vicinity of the transition to reduce the accelerations and the forces in the elements of the railway superstructure. In the case of a ballasted track-slab track transition, Giannakos and Tsoukantas (2012) presented a new method to calculate the contact force between the sleepers and the ballast and compared it with others already existing, studying the variation of the static and dynamic stiffness in the transition zone as well.

## 2. Description of the Studied Track

The studied track is located in the L1 line of the Alicante TRAM network, near Poble Espanyol station. In this location, the dynamic and structural behavior of a new slab track developed with asphalt mixtures containing recycled aggregates in the dosage and designed specifically to provide a high performance against vibrations induced by railway vehicles is assessed. To study this new slab track, a 20 m stretch was placed in an existing transition between a ballasted track and a concrete slab track. Thus, the final result was a line stretch made of three different track typologies and two transitions between them, which will be modeled and comprehensively studied in the following sections.

Fig. 1. Detail of the 20 m Stretch of Asphalt Slab Track Inserted between the Previously Existing Concrete Slab Track and Ballasted Track

### 2.1 Sections and Materials

Since a 3D finite element model is necessary to study the transitions between the different track typologies, it is important to know the detailed geometry of the real infrastructure from which the model is created.

In the ballasted track, the ballast is placed directly on the natural sandy ground. The concrete monoblock sleepers lie on the ballast layer and give support to the UIC-54 rails, with a railpad placed in between as depicted in Fig. 2(a). This track type

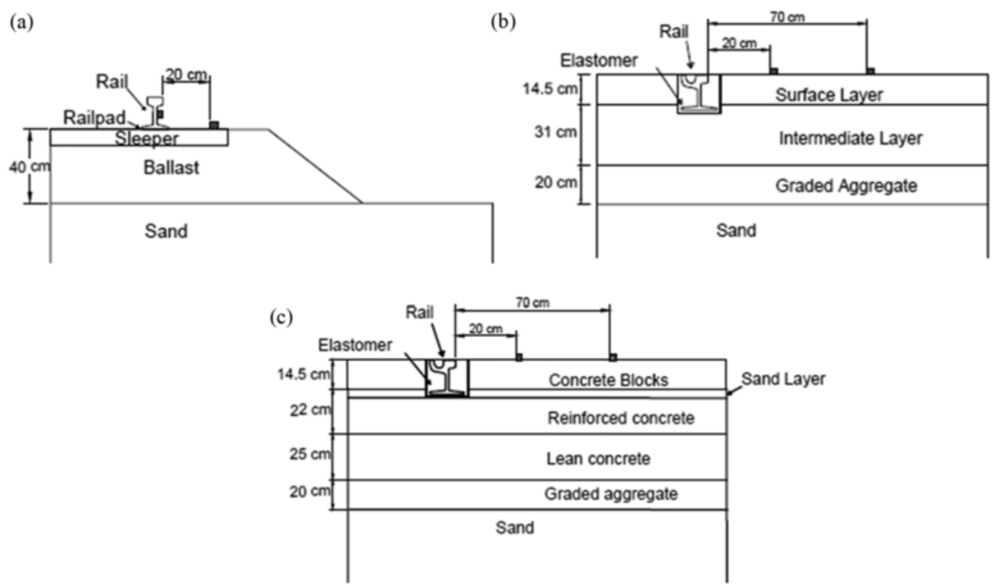


Fig. 2. Cross Section of the Different Track Typologies

Table 1. Mechanical Properties of the Materials in the Three Track Typologies

| | | E (MPa) | $\nu$ | $\rho$ (kg/m$^3$) | $\beta_{Rayleigh}$ |
|---|---|---|---|---|---|
| Ballasted Track | Railpad | 178,6 | 0,3 | 900 | 0,00063 |
| | Sleeper | 27000 | 0,25 | 2400 | 0,00003152 |
| | Ballast | * | 0,3 | 1900 | $\beta_B$ |
| Bituminous Slab Track | Elastomer | 26,7 | 0,48 | 900 | 0,00063 |
| | Asphalt Mixture | 11500 | 0,33 | 2400 | $\beta_{AM}$ |
| Concrete Slab Track | Elastomer | 26,7 | 0,48 | 900 | 0,00063 |
| | Paving Blocks | 2250 | 0,25 | 2400 | 0,00003152 |
| | Sand layer | 30 | 0,3 | 1800 | $\beta_C$ |
| | Reinforced Concrete | 27300 | 0,25 | 2400 | 0,00003152 |
| Common Elements | Rail | 210000 | 0,3 | 7850 | 0,00003152 |
| | Graded Aggregate | 171 | 0,3 | 1700 | $\beta_{GA}$ |
| | Sand | 120 | 0,3 | 2000 | $\beta_S$ |

is linked to the asphalt slab track represented in Fig. 2(b) in which a change to a Ph37N grooved rail embedded in elastomer is observed. The surface and intermediate layers are made of a SMA16 asphalt mixture with a 0.5% of recycled plastics and rest on a 20 cm thick layer of graded aggregate placed on the natural soil. The concrete slab track represented in Fig. 2(c) shares the graded aggregate layer with the adjacent asphalt slab track but a lean concrete bed is placed on this instead to support the reinforced concrete layer. Finally, a thin sand layer is placed under the surface concrete blocks and the reinforced concrete.

In addition to the cross section geometries, it is important to know the mechanical properties of the different materials. These properties, which will also become model inputs, are summarized in Table 1.

The elasticity modulus of the ballast is represented by an asterisk because this value is a priori unknown. Moreover, some values of the Rayleigh damping coefficients β have been obtained from Fernández (2014) but there are others which are particular of the studied case. In the calibration process developed in section 3, these unknown parameters will be estimated using real acceleration records.

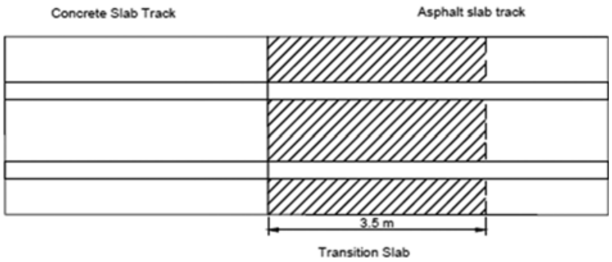


Fig. 3. Plan View of Transition 1

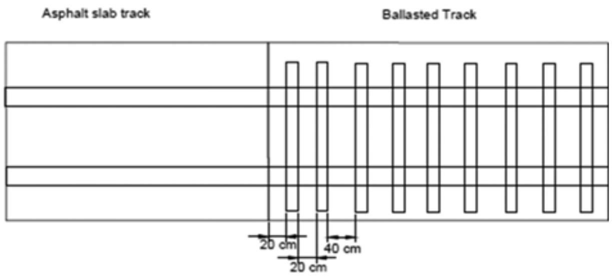


Fig. 4. Plan View of Transition 2

### 2.2 Existing Transitions

As can be guessed from the information in Table 1, the concrete slab track will have the highest vertical stiffness, followed by the asphalt slab track and the ballasted track. For this reason, different measures addressed to lessen the abrupt stiffness change were taken during the construction of the infrastructure.

#### 2.2.1 Transition 1: Asphalt Slab Track-concrete Slab Track

The stiffness difference existing in this case is not as marked as in transition 2. Even so, a lean concrete transition was executed between the graded aggregate and the intermediate layer of the asphalt slab track. This transition slab shown in Fig. 3, is 15 cm thick and 3.5 m long in the direction of the track.

#### 2.2.2 Transition 2: Ballasted Track-asphalt Slab Track

With the objective of increasing the stiffness of the ballasted track in the transition vicinity, the distance between the two sleepers closer to the asphalt slab track was reduced as shown in Fig. 4. These sleepers were placed at a distance of 20 cm, instead of the 40 cm existing in the rest of the line to allow the tamping operations.

Decreasing gradually the separation between the sleepers near the transition to a stiffer track is an effective manner to avoid the sudden stiffness change and its negative effects on the track and the vehicle.

### 2.3 Experimental Campaign

Six three-axial Sequoia Fast Tracer™ accelerometers were used in the experimental campaign. Technical specifications of these devices are summarized in Table 2.

Each of the three track typologies was monitored with a pair of accelerometers as indicated by squares in Fig. 2. Since the base of the accelerometers is magnetic, a metal plate was fixed to the sleeper and slab surfaces using epoxy adhesive. Devices were located in the transition zones: on two different sleepers (one in

Table 2. Technical Specifications of the Accelerometers

| | |
|---|---|
| Scope (g) | ±2 |
| Bandwidth (Hz) | 0-2500 |
| Resolution (m/s2) | 0.041 |
| Noise (m/s2) | 0.075 |
| Sampling Rate (Hz) | 8192 |

the transition zone) for the ballasted track and at a distance of 0.2 and 0.7 m measured from the outer side of the rail for transitions in concrete and asphalt slab tracks. In this manner, acceleration at six different points, located in three different tracks, was simultaneously measured during the train passages.

During the experimental campaign, a total number of 17 train passages were recorded. These passages correspond to the vehicle Vossloh 4100, whose technical characteristics can be consulted in Real *et al.* (2014), running at a speed between 33-36 km/h. Registers corresponding to the first three passages were used to adjust the accelerometers. Among the remaining 14 data records, it was not observed any significant difference in any of the six monitored points. Consequently, six random registers were chosen to calibrate and validate the FEM model.

## 3. Finite Elements Model of the Studied Track

The three-dimensional finite elements model of the studied track in Fig. 5 has been constructed using the software ANSYS v14. In this scheme, the geometry of the different sections described in Fig. 2 is represented and the transitions shown in Figs. 3 and 4 have been implemented as well. The elements chosen for the analysis are SOLID45, with the mechanical properties presented in Table 1. The total length of the model is 60m, divided in 3 stretches of the same length correspondent to each track typology. Two different analyses are run on this model: one dynamic to obtain the accelerations induced by the train loads passage and another static to calculate the deflections caused by these loads and, subsequently, the vertical track stiffness.

The considered load corresponds to that transmitted by the considered vehicle, carrying 4 passengers per square meter in each of the three carriages. The final load result (90 kN/axle) has been incremented to include the dynamic overloads according to the German criterion explained in Fastenrath (1981). The final load is 63.95 kN/wheel considering medium track conditions and high statistical precision (95.5%). Vehicle speed has been set in 35 km/h since all the real registers were measured when the trains run at speeds of 33-36 km/h. More complex models of track-vehicle interaction exist in the literature to include the dynamic effects as the one presented by Yang *et al.* (2009) for stress calculation in the track support considering the rail profile; the model described in Jin *et al.* (2006) to determine the force transmitted by the train as a function of the track geometry and including rail corrugation and finally, the model created by Ferrara *et al.* (2012) to calculate accelerations taking into account the corrugation and the wheel flats. However, since the objective of this research is the study of the static and dynamic behavior of the transitions, it is only considered the effect of the incremented quasi-static load which will allow the assessment of the proposed scenarios in a simple manner and with enough accuracy. As pointed by Shan *et al.* (2013), this simplification that does not attend the vehicle-track interaction is not totally representative of the real dynamic behavior and becomes a major limitation of the model. Nevertheless, the high level of detail of the track 3D FEM model is more realistic than those characteristic of the vehicle-track coupled models where the different track components and the soil are represented by spring-damper systems.

Moreover, the results obtained from the dynamic analysis will be compared with real acceleration registers measured at different points of the studied track in order to obtain the elasticity modulus of the ballast, which was unknown, and the damping parameters of the different track typologies. Monitored points, at which accelerations are compared, have been defined in section 2.3 and their location is represented by squares in Fig. 2.

### 3.1 Calibration for the Estimation of the Ballast Elasticity Modulus and the Damping Parameters

The dynamic analysis performed to obtain the unknown parameters is based on the Rayleigh damping theory, thoroughly

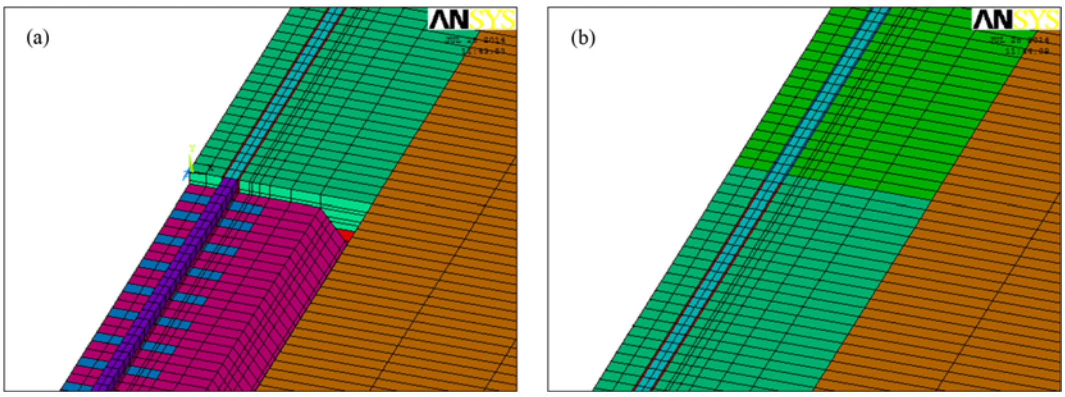


Fig. 5. FEM Model of the Studied Track. Detail of the Transition Ballasted Track-asphalt Slab Track: (a) and Asphalt Slab Track-concrete Slab Track (b)

explained in Real *et al.* (2014) and Real *et al.* (2012). This theory considers a global damping parameter $\beta$, which is characteristic of each track section. Therefore, in the FEM model described in this work will take three different values: $\beta_{ballasted}$, $\beta_{asphalt}$ and $\beta_{concrete}$. The consideration of a global $\beta$ coefficient for each track typology allows reducing the number of unknowns in Table 1 from 6 to 4 since $\beta_{ballasted}$ includes $\beta_B$, $\beta_{GA}$ and $\beta_S$; $\beta_{asphalt}$ accounts for $\beta_{AM}$, $\beta_{GA}$ and $\beta_S$ and $\beta_{concrete}$ comprises $\beta_C$, $\beta_{GA}$ and $\beta_S$.

These three unknowns, plus the ballast elasticity modulus, have been determined from the real acceleration records measured on the sleeper ($E_{ballast}$ and $\beta_{ballasted}$); at a distance of 0.2 m from the rail on the transition zone of the asphalt concrete layer ($\beta_{asphalt}$) and at a distance of 0.7 m from the rail on the concrete slab track, also close to the transition ($\beta_{concrete}$). To calculate these parameters, the FEM model is run after assigning random values to these parameters within an expected range. After obtaining the vibration response, this is compared with the real registers at the same points, considering as the solution those values which yield the accelerogram closer to the real response. The results from this process to obtain the unknown parameters are shown in Fig. 6.

Plots in Fig. 6 have been calculated using $E_{ballast}$ = 30 MPa; $\beta_{ballasted}$ = 0.0005; $\beta_{asphalt}$ = 0.0005 and $\beta_{concrete}$ = 0.001. As it has been only considered the effect of the quasi-static load transmitted by each vehicle axle, the accelerograms calculated by the model represent exclusively the effect produced by these forces.

The predicted peak values produced by these loads are very similar to the records of the three studied track typologies, in which the effect of each of the four bogies of the vehicle is clearly identified. On the other hand, since the dynamic forces are not specifically considered (e.g., those caused by irregularities in the wheel-rail contact surface) but the quasi-static load has been incremented, the accelerations linked to these forces that complete the real acceleration data sets with lower amplitudes and higher frequencies have not been predicted by the model.

### 3.2 Model Validation

It is necessary to ensure that the values determined in the previous subsection of the unknown parameters are not only valid for the points where they have been calculated but they are representative of the global behavior of the structure. For this reason, the accelerations at the transition sleeper and at a distance

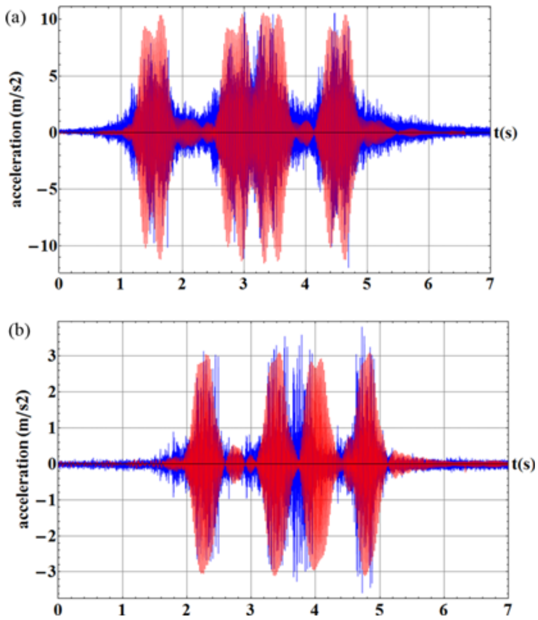


Fig. 7. Validation of the 3D FEM Model on the Transition Zones of the Ballasted Track (a) and the Asphalt Slab Track, (b) Original Registers are Displayed in Blue and FEM Model Results in Red

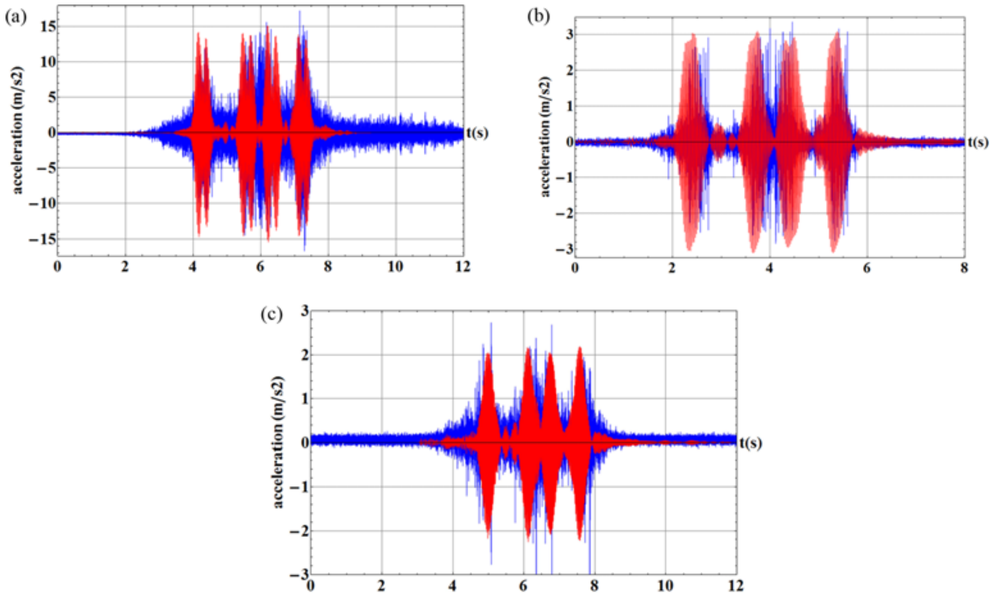


Fig. 6. Calculation of the Unknown Parameters for the Ballasted Track: (a) Asphalt Slab Track, (b) and Concrete Slab Track (c). Original Registers are Displayed in Blue and FEM Model Results in Red

of 0.7 m of the outer side of the rail on the asphalt slab track, just over the transition lean concrete slab are calculated. By comparing these predicted accelerograms with acceleration data sets from the real track, the accuracy of the model is evidenced as well as the validity of the values calculated for the unknowns of each track typology in the studied track.

As deduced from Fig. 7, when the model is run considering the parameters calculated in section 3.1, the predicted responses at the different track points are still valid. The maximum values predicted at the considered points of each transition are of the same magnitude and the acceleration responses corresponding to the passage of the vehicle bogies match in the time scale. As in the calibration process, the only vibration generation mechanism considered is the effect of the quasi-static load which explains some of the differences existing between the calculated and the real response.

## 4. Evaluation of Improvements for the Transition Design

As previously explained, the most important property that the transition must fulfill is to provide a progressive variation of the track vertical stiffness. In this section, three different methods existing in the literature to achieve a gradual stiffness transition are analyzed: the implementation of additional rails in the ballasted track; the variation of the elastomers' stiffness and the placement of resilient mats in the infrastructure.

From the FEM model developed in section 3, both the static (stiffness) and dynamic (acceleration) responses will be calculated on the track in the different scenarios considered. Comparing the obtained results with those from the original track configuration, the contribution of the different elements considered to achieve a smoother transition can be assessed as well as their influence on the dynamic behavior of the track.

### 4.1. Vertical Stiffness of the Original Track

In this subsection, the deflections produced by a passing load are calculated running a static analysis. If the load that produces the deflection is divided by this calculated displacement in every point of the modeled track, the vertical stiffness for the three track typologies and the two transitions is obtained.

The results plotted in Fig. 8 show the stiffness variation. The interval [10-20] m corresponds to the concrete slab track, with a notable high vertical stiffness around 270 kN/mm. After the 20 m extreme begins the asphalt slab track, which is 20 m long, with a stiffness of 180 kN/mm. At the end of the asphalt slab track, the stiffness drops again to 71 kN/mm in the ballasted track and keeps this value until the distance 50 m. The graph in Fig. 8 considers only the central 40 m of the model in order to avoid the influence of the boundaries on the stiffness results, assuming that the extreme values remain constant in the intervals [0-10] m and [50-60] m.

Transition 2 between the asphalt slab track and the ballasted track is more pronounced because here there is a larger stiffness difference and higher slope than in the case of the transition 1 between the concrete slab track and the asphalt slab track.

### 4.2 Change of the Stiffness of the Elastomers

The influence of the railpads on the accelerations and the dynamic loads produced in transitions between slab track and ballasted track was studied by Lei and Hang (2011). These authors concluded that the stiffness of the elastomers influenced the global vertical stiffness of the track and, consequently, the forces acting on the rail and the registered accelerations.

The substitution of the elastomers is an extremely effective method to modify the vertical stiffness of the track due to its simplicity, even when the track is operating. For this reason, two different changes addressed to the achievement of a smoother transition than the currently existing are studied in this section. Firstly, the stiffness of the concrete slab track will be reduced by changing the elastomer in which the rail is embedded for other more elastic (60 kN/mm against the existing 100 kN/mm). The elastic elastomer will be placed along three meters from the transition section. At the same time, the stiffness of the ballasted track near the transition is increased in the following manner: the railpads over the two sleepers closer to the transition will be 500 kN/mm stiff; the following three railpads 250 kN/mm and the rest will maintain the original stiffness of 100 kN/mm.

From the results in Fig. 9, it can be deduced that the transition has been improved between the concrete and the asphalt slab tracks after the substitution of the elastomer in which the rail is embedded by other more elastic. On the other hand, the change of the railpads in transition 2 does not yield the expected results and the stiffness variation is as the original, being the graphs

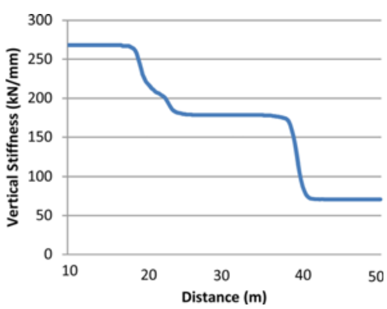


Fig. 8. Stiffness Evolution Along the Three Different Track Typologies Studied

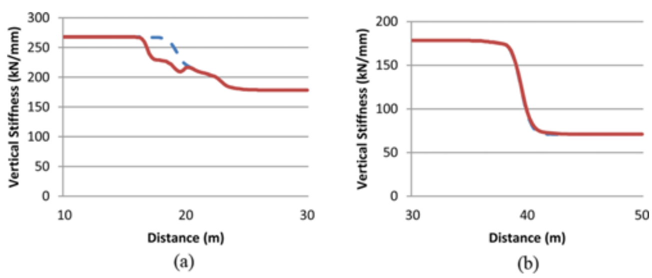


Fig. 9. Evolution of the Track Vertical Stiffness at Transition 1 (a) and at Transition 2 (b) After the Change of the Stiffness of the Elastomers. Dashed Line Represents the Original Results

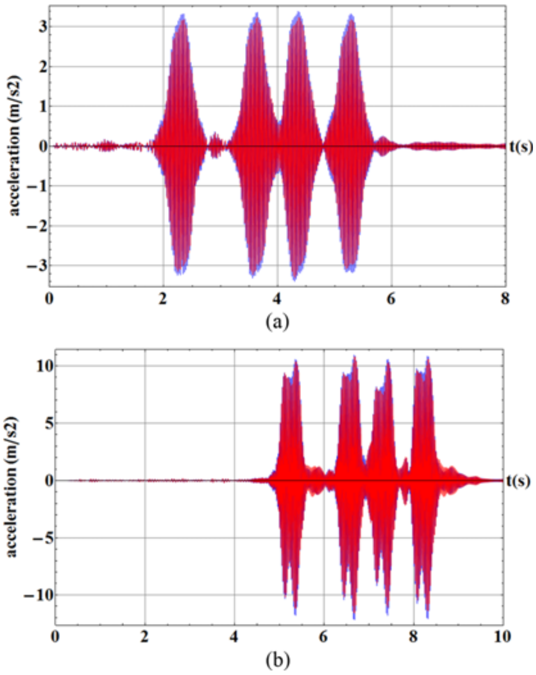


Fig. 10. Calculated Accelerations at 0.2 m from the Rail Side on the Concrete Slab Track: (a) and on the Transition Sleeper, (b) before (red) and after (blue) the Change of the Stiffness of the Elastomers

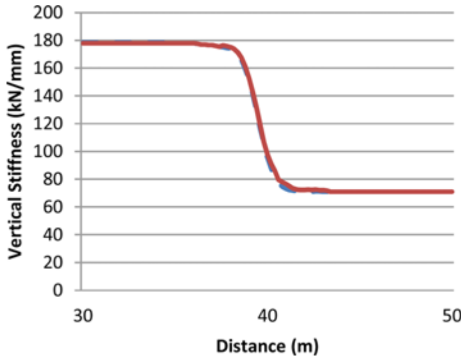


Fig. 11. Effect of the Additional Rails in Transition 2 on Vertical Stiffness. Dashed Line Represents the Original Results

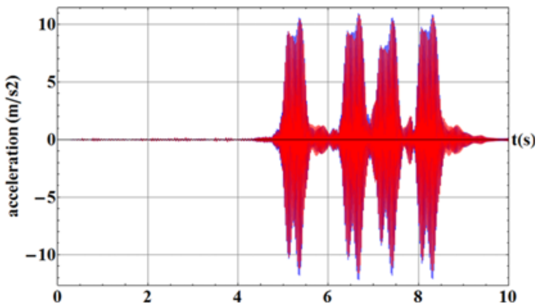


Fig. 12. Calculated Accelerations on the Transition Sleeper before (red) and after (blue) the Inclusion of the Additional Rails

totally overlapped.

The dynamic behavior of the track after the changes is shown in Fig. 10. According to the previously said, the vibration responses in transition 2 are almost identical while in transition 1, the acceleration slightly increases when a more elastic elastomer is considered.

### 4.3 Additional Rails on the Ballasted Track

This simple strategy to increase the stiffness is studied in Kerr and Moroney (1995) and consists of two additional parallel rails fixed to the sleepers between the rails on which the train moves. In the studied case, the existing rails were duplicated, implementing in the model two segments 3 m long of UIC-54 rails at a distance of 0.2 m from the axis of the ballasted track at the transition zone. This measure results very useful since it can be performed in an operating track without affecting the infrastructure. However, it is only suitable for ballasted tracks.

There is no evidence of improvement after the implementation of the additional rails what may suggest that the previous transition, in which the distance between sleepers was reduced, was properly designed. However, track stiffness along the transition is higher after the extra rails placement (the continuous line is always over the dashed one at the transition). Regarding the dynamic response, it is observed how in a stiffer transition the acceleration peaks on the sleeper decrease slightly for the same loading condition. This acceleration diminution brings with a lower deterioration rate of the ballast layer in the transition vicinity, thus expanding the life span of the infrastructure.

### 4.4 Resilient Mats

The use of resilient mats was studied by Xin and Gao (2011) in floating slab tracks on bridges and Costa *et al.* (2012) in ballasted tracks. Both researches concluded that the vibration isolation was better when the elasticity of the mats increased but this had negative consequences: too elastic mats may cause excessive movements of the slab and the rail. Moreover this alternative cannot be implemented in an operating line as easy as the railpads or the additional rails studied before, which means an important drawback.

In the studied case, two resilient mats of different stiffness will be placed between the graded aggregate and the reinforced concrete layer in the transition 1 and under the ballast in the transition 2. The objective is to diminish the vertical stiffness of the concrete slab track and increase it in the ballasted track at the transition zones respectively. Therefore, the stiffness of the mats will be 100 kN/mm for transition 1 and 500 kN/mm in transition 2, being the length of the mats 3 m from the transition sections.

As in the previous cases analyzed in subsections 4.2 and 4.3, transition 2 between the asphalt slab track and the ballasted track is not affected by the changes performed. On the other hand, the high-elasticity mat placed in the concrete slab track produces a stiffness reduction in this zone achieving a smooth transition as seen in Fig. 13. The stiffness variation results in three steps of stiffness reduction along the transition. Analogously, the vibration response of the sleepers remains unchanged while on the surface of the concrete slab the acceleration increases as a consequence of the low stiffness of the mat (see Fig. 14), which is in total

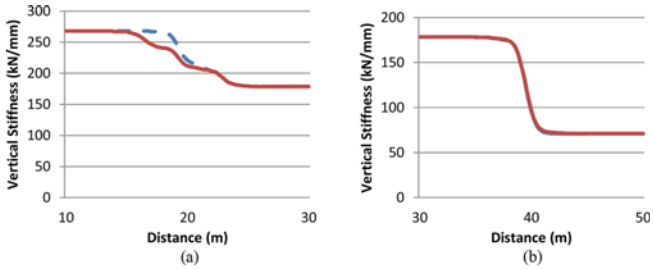


Fig. 13. Evolution of the Track Vertical Stiffness at Transition 1, (a) and at Transition 2, (b) after the Placement of the Resilient Mats. Dashed Line Represents the Original Results

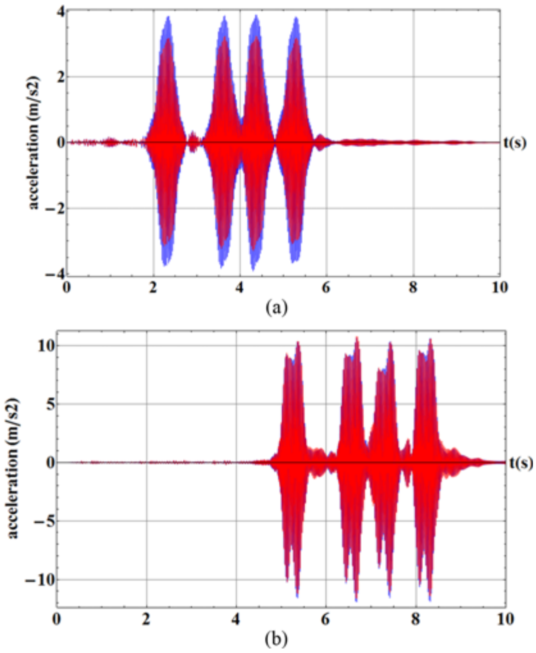


Fig. 14. Calculated Accelerations at 0.2 m from the Rail Side on the Concrete Slab Track (a) and on the Transition Sleeper, (b) before (red) and after (blue) the Implementation of the Resilient Mats

agreement with the literature findings presented before.

## 5. Conclusions

Two different transitions have been analyzed in this study. These transitions were located between three different track typologies: ballasted track; asphalt slab track and concrete slab track. To perform the analysis, a three-dimensional finite elements model has been developed and validated with real acceleration measurements. From this model, a static analysis has been run in order to determine the evolution of the stiffness along the transition. Moreover, a dynamic analysis has also been executed to study the accelerations in the different scenarios.

The results of the FEM model have revealed the following results:

1. The stiffness slope in the transition zone between a concrete and an asphalt slab track can be improved either reducing the elastomer stiffness in the concrete slab track or using resilient mats under the concrete slab track.
2. Additional rails on the ballasted track do not contribute achieve a smoother transition. The sole reduction of the sleeper spacing in the sleepers closer to the transition is recommended instead.
3. Neither the elastomer stiffness nor the resilient mats have improved the transition behavior between asphalt and concrete slab tracks. In the cases in which the stiffness slope is too acute, it would be convenient to increase the length of the transition slab located beneath the asphalt slab track; it means that the existing track has to be removed to build the new transition slab, affecting in this manner to the line operation.

The dynamic behavior of the infrastructure does not significantly vary since the accelerations are very similar in the different scenarios considered. Only when an elastic resilient mat is placed under the concrete slab track, the accelerations on the track surface increase slightly. In this regard, it must be considered that only the form in which this stiffness is distributed along the transition changes, not the values. Consequently, the vibration response at these points of the transition is not altered.

## Acknowledgements

This research is included within the Research and Development project BITUTRAN supported by the CDTI (Center for the Industrial Technological Development) of the Spanish Ministry of Economy and Competitiveness. The contribution of EIGE (Infrastructure Authority of the Regional Government of Valencia) and FGV (Railways of the Valencia Region) during the development and the implementation of the project must be acknowledged.

## References

Ali Zhakeri, J. and Ghorbani, V. (2011). "Investigation on dynamic behavior of railway track in transition zone." *Journal of Mechanical Science and Technology,* Vol. 25 No. 2, pp. 287-292, DOI: 10.1007/s12206-010-1202-x.

Coelho, B., Hölscher, P., Priest, J. P., and Barends, F. (2011). "An assessment of transition zone performance." *Journal of Rail and Rapid Transit*, Vol. 225, No. 2, pp. 129-139, DOI: 10.1177/09544097JRRT389.

Costa, P. A., Calçada, R., and Cardoso, A. (2012). "Ballast mats for the reduction of railway traffic vibrations. Numerical study." Soil *Dynamics and Earthquake Engineering*, Vol. 42, pp. 137-150, DOI: 10.1016/j.soildyn.2012.06.014.

Fastenrath, F. (1981). *Railroad Track: Theory and practice: material properties*, cross sections, welding and treatment, F. Ungar Pub. Co., New York, N.Y.

Fernández, J. (2014). *Numerical study in time domain of the vibrations induced by railway traffic in tunnels: Geotechnical analysis, experimental validation and solutions proposal,* PhD Thesis, University of La Coruña, Spain. (In Spanish).

Ferrara, R., Leonardi, G., and Jourdan, F. (2012). "Numerical Modelling of Train Induced Vibrations." *Proc. 5th International Congress on Sustainability of Road Infrastructures. Procedia-Social and Behavioral*

*Sciences*, Rome, pp.155-165, DOI: 10.1016/j.sbspro.2012.09.869.

Gallego Giner, I., Vieira Chaves, E. W., López Pita, A., and Rivas Álvarez, A. (2012). "Design of embankment-structure transitions for railway infrastructure." *Transport*, Vol. 165, No. 1, pp. 27-37, DOI: 10.1680/tran.8.00037.

Giannakos, K. and Tsoukantas, S. (2012). "Transition zone between ballastless and ballasted track: Influence of changing stiffness on acting forces." *Transport Research Arena 2012. Procedia-Social and Behavioral Sciences*, Vol. 48, pp. 3548-3557, DOI: 10.1016/j.sbspro.2012.06.1318.

Jin, X. S., Wen, Z. F., Wang, K. Y., Zhou, Z. R., Liu, Q. Y., and Li, C. H. (2006). "Three-dimensional train-track model for study of rail corrugation." *Journal of Sound and Vibration*, Vol. 293, Nos. 3-5, pp. 830-855, DOI: 10.1016/j.jsv.2005.12.013.

Kerr, A. and Moroney, B. (1995). "Track transition problems and remedies." *American Railway Engineering Association*, Vol. 742, pp. 267-297.

Lei, X. and Zhang, B. (2011). "Analysis of dynamic behavior for slab track of high-speed railway based on vehicle and track elements." *Journal of Transportation Engineering*, Vol. 137, No. 4, pp. 227-240, DOI: 10.1061/(ASCE)TE.1943-5436.0000207.

Li, D. and Davis, D. (2005). "Transition of railroad bridge approaches." *Journal of Geotechnical and Geoenvironmental Engineering*, Vol. 131, No. 11, pp. 1392-1398, DOI: 10.1061/(ASCE)1090-0241(2005)131:11(1392).

Real, J., Galisteo, A., Real, T., and Zamorano, C. (2012). "Study of wave barriers design for the mitigation of railway ground vibrations." *Journal of Vibroengineering*, Vol. 14, No. 1, pp. 408-422.

Real, J., Zamorano, C., Hernández, C., Comendador, R., and Real, T. (2014). "Computational considerations of 3-D finite element method models of railway vibration prediction in ballasted tracks." *Journal of Vibroengineering*, Vol. 16, No. 4, pp. 1709-1722.

Shan, Y., Albers, B., and Savidis, S. (2013). "Influence of the different transtion zones on the dynamic response of track-subgrade systems." *Computers and Geotechnics*, Vol. 48, pp. 21-28, DOI: 10.1016/j.compgeo.2012.09.006.

Shi, J., Burrow, M., Chan, A. H., and Wang, Y. J. (2012). "Measurements and simulation of the dynamic responses of a bridge-embankment transition zone below a heavy haul railway line." *Journal of Rail and Rapid Transit*, Vol. 227, No. 3, pp. 254-268, DOI: 10.1177/0954409712460979.

Varandas, J., Hölscher, P., and Silva, M. (2011). "Dynamic behaviour of railway tracks on transtion zones." *Computers and Structures*, Vol. 89, Nos. 13-14 pp. 1468-1479, DOI: 10.1016/j.compstruc.2011.02.013.

Witt, S. (2008). *The influence of under sleeper pads on railway track dynamics,* Linköping University, Linköping.

Woodward, P. K., El Kacimi, A., Laghrouche, O., Medero, G., and Banimahd, M. (2012). "Application of polyurethane geocomposites to help maintain track geometry for high-speed ballasted railway tracks." *Journal of Zhejiang University-Science A*, Vol. 13, No. 11, pp. 836-849, DOI: 10.1631/jzus.A12ISGT3.

Xia, J. H. Wei, Q. C. Yin, S., and You, L. X. (2009). "Dynamic performance evaluation of bridge-subbgrade transition of Shuohuang Railway." *Proc. of 2010 International Conference on Measuring Technology and Mechatronics Automation, Changsha City*, Vol. 2, pp. 58-61, DOI: 10.1109/ICMTMA.2010.605.

Xin, T. and Gao, L. (2011). "Reducing slab track vibration into bridge using elastic materials in high speed railway." *Journal of Sound and Vibration*, Vol. 330, No. 10, pp. 2237-2248, DOI: 10.1016/j.jsv.2010.11.023.

Yang, L., Powrie, W., and Priest, J. (2009). "Dynamic stress analysis of a ballasted railway track bed during train passage." *Journal of Geotechnical and Geoenvironmental Engineering*, Vol. 135, No. 5, pp. 680-689, DOI: 10.1061/_ASCE_GT.1943-5606.0000032.

Zhang, B., Zhao, X., and Liu, Q. (2013). "Calculation and evaluation on dynamic characteristics of bridge-subgrade transition section in speed-up railway line." Applied Mechanics and Materials, Vols. 256-259, pp. 1821-1825, DOI: 10.4028/www.scientific.net/AMM.256-259.1821.